Role of stacking fault energy on texture evolution revisited

R Madhavan[1], R Kalsar[1], RK Ray[2] and S Suwas[1]
[1] Department of Materials Engineering, Indian Institute of Science, Bangalore 560012, India
[2] Formerly Professor, Department of Metallurgical and Materials Engineering,
Indian Institute of Technology, Kanpur 208016, India
E-mail: satyamsuwas@materials.iisc.ernet.in

Abstract. Three materials, pure aluminium, Al-4 wt.% Mg, α-brass have been chosen to understand the evolution of texture and microstructure during rolling. Pure Al develops a strong copper-type rolling texture and the deformation is entirely slip dominated. In Al-4Mg alloy, texture is copper-type throughout the deformation. The advent of Cu-type shear bands in the later stages of deformation has a negligible effect on the final texture. α-brass shows a characteristic brass-type texture from the early stages of rolling. Extensive twinning in the intermediate stages of deformation ($\varepsilon_t \sim 0.5$) causes significant texture reorientation towards α-fiber. Beyond 40% reduction, deformation is dominated by Bs-type shear bands, and the banding coincides with the evolution of <111>||ND components. The crystallites within the bands preferentially show <110>||ND components. The absence of the Cu component throughout the deformation process indicates that, for the evolution of brass-type texture, the presence of Cu component is not a necessary condition. The final rolling texture is a synergistic effect of deformation twinning and shear banding.

1. Introduction

The transition of deformation texture from copper-type to brass-type as a function of stacking fault energy (SFE) in fcc metals and alloys is a subject of investigation spanning over five decades [1]. Material with high/medium SFE develops a copper-type texture on rolling, while a brass-type texture is common in low-SFE material. Typically, a copper-type texture comprises equal fractions of copper (Cu) {112}<111>, brass (Bs) {110}<112> and S {123}<634> orientations, whereas a brass-type texture primarily consists of Bs and Goss {110}<001> components with negligible Cu fraction. It was earlier proposed that this texture change is attributed to the extent of cross slip, where easy cross slip (high SFE) leads to copper-type texture and otherwise to brass-type texture [2]. However, it was later suggested that the evolution of the brass-type texture in low SFE materials is related to deformation twinning [3]. Many experimental outcomes have indicated that the rolling texture in a low-SFE fcc material is similar to that of a high-SFE material up to certain deformation levels (~40%) and the deviation from copper-type to brass-type occurs only at the later stages of deformation [4,5]. It is argued that this transition is due to selective twinning in Cu-oriented grains. However, Leffers and co-workers [6,7] have noted clear differences between the two types of rolling textures from the early deformation stages. Further, Leffers [8] argued that twinning does not play a direct role in the evolution of the brass-type texture, but has an indirect effect. The dislocation slip subsequent to twinning is greatly hindered since the twin boundaries could act as obstacle for dislocation motion and hence slip would be confined to planes parallel to the twin habit plane.

It has been observed experimentally that the propensity for twinning ceases at intermediate levels of deformation and is followed by subsequent formation of shear bands at higher reductions. Shear bands can be either Cu-type (which are common in high- and medium-SFE materials and form as a result of increased obstruction to dislocation motion due to preexisting dislocation cell walls and micro-bands) [9] or Bs-type (common in low-SFE materials and are observed to form when the preceding obstacles are twin lamellae) [10]. In high- and medium-SFE materials, activity of shear bands has been observed only at very large deformation, when the texture is predominantly Cu-type. In Cu-Mn alloys, Engler [11] found

that the volume of shear-banded regions in the microstructure increased with deformation and these microscopic shear bands were selectively found in grains having Cu orientation. In Al-Cu and Al-Mg alloys [12,13], where the formation of Cu-type shear bands is extensive at the later stages of deformation, it can be seen that the orientations of sub-grains within shear bands have hardly any effect on the final Cu-type rolling texture. On the other hand, in low-SFE material, subsequent to twinning, a continuous slip preferentially on twin habit planes rotates the {111} crystal plane parallel to the rolling plane [14]. This makes homogeneous deformation difficult and results in shear banding. The concurrence of the evolution of <111>||ND components and the origination of shear bands has been observed in many low-SFE materials [15,16]. These Bs-type shear bands are observed to form preferentially in grains with <111>||ND orientation [17]. In Cu-30Zn alloy, Duggan et al. [16] observed that the volume fraction of shear bands is large and has a significant role in the final texture. It is to be noted that in all the above studies, irrespective of the type of shear bands and SFE values, it has been reported that the crystallites within the bands have orientations close to <110>||ND.

In a recent work by the authors, the transition of texture from copper-type to brass-type has been observed at very large strain in a medium-SFE Ni-40Co alloy [18]. This texture deviation is attributed to the extensive activity of Cu-type shear bands preferentially in Cu-oriented grains. However, in low-SFE Ni-60Co alloy, the formation of brass-type texture initiates at the early stages of deformation, and it is observed that deformation twinning and Bs-type shear banding have a synergistic effect on the final texture [19]. The present study is aimed to understand the general trend in the evolution of microstructure and crystallographic texture as function of SFE in a range of fcc materials exhibiting different SFE values. A representative material from each of high-SFE (pure aluminum), medium-SFE (Al–4Mg) and low-SFE (Cu–30Zn) regimes has been chosen and its texture-microstructure correlation has been presented.

2. Experimental

The cast ingots of ultra pure Al (99.9999%), Al-4 wt.% Mg and Cu-30 wt.% Zn (α-brass) were obtained by vacuum melting. In order to weaken the initial texture, the ingots were subjected to 50% cross rolling followed by annealing at $0.5T_m$ for 6 h. The average grain size of the starting material is about 150 μm. The initial material has been cold rolled to 98% thickness reduction (equivalent true strain – 3.99). Textures for the initial and the cold rolled samples have been measured using Bruker D8 Discover texture goniometer with Cu K_α radiation. Four incomplete pole figures ($\alpha = 0 – 75^o$, $\Delta\alpha = 5^o$) of 111, 200, 220, 311 planes have been measured on the normal plane mid-thickness section. The Orientation Distribution Function (ODF) has been calculated from the measured pole figures using MTex software [20], which is available as MATLAB toolbox. Orthotropic sample symmetry has been imposed for the texture of rolled samples. The microstructural characterization for the rolled samples was done using a scanning electron microscope attached with an electron back-scattered diffraction (EBSD) camera. All the EBSD scans were taken on the transverse plane of the rolled sample.

3. Results

3.1 Evolution of texture

The $\varphi_2 = 0°, 45°, 65°$ sections of the ODF are shown for the 70%, 95% and 98% cold rolled conditions in Fig. 1. The presence of a strong <110>||ND texture is evident in the $\varphi_2 = 0°$ section in all materials at higher strain levels. For pure Al and Al-4Mg, the maximum intensity (in terms of f(g)) is seen near to Bs ($\varphi_1 = 35°$) locations (Figs. 1a, b). On the other hand, in α-brass, no unique intensity maximum is seen (Fig. 1c). Apart from the <110>||ND components, the simultaneous evolution of Cu and S components can be

observed in the φ_2 = 45° and 65° sections, respectively, in pure Al and Al-Mg alloy. On the contrary, in α-brass, the evolution of brass-type texture is associated with a complete absence of Cu-component in the φ_2 = 45° section.

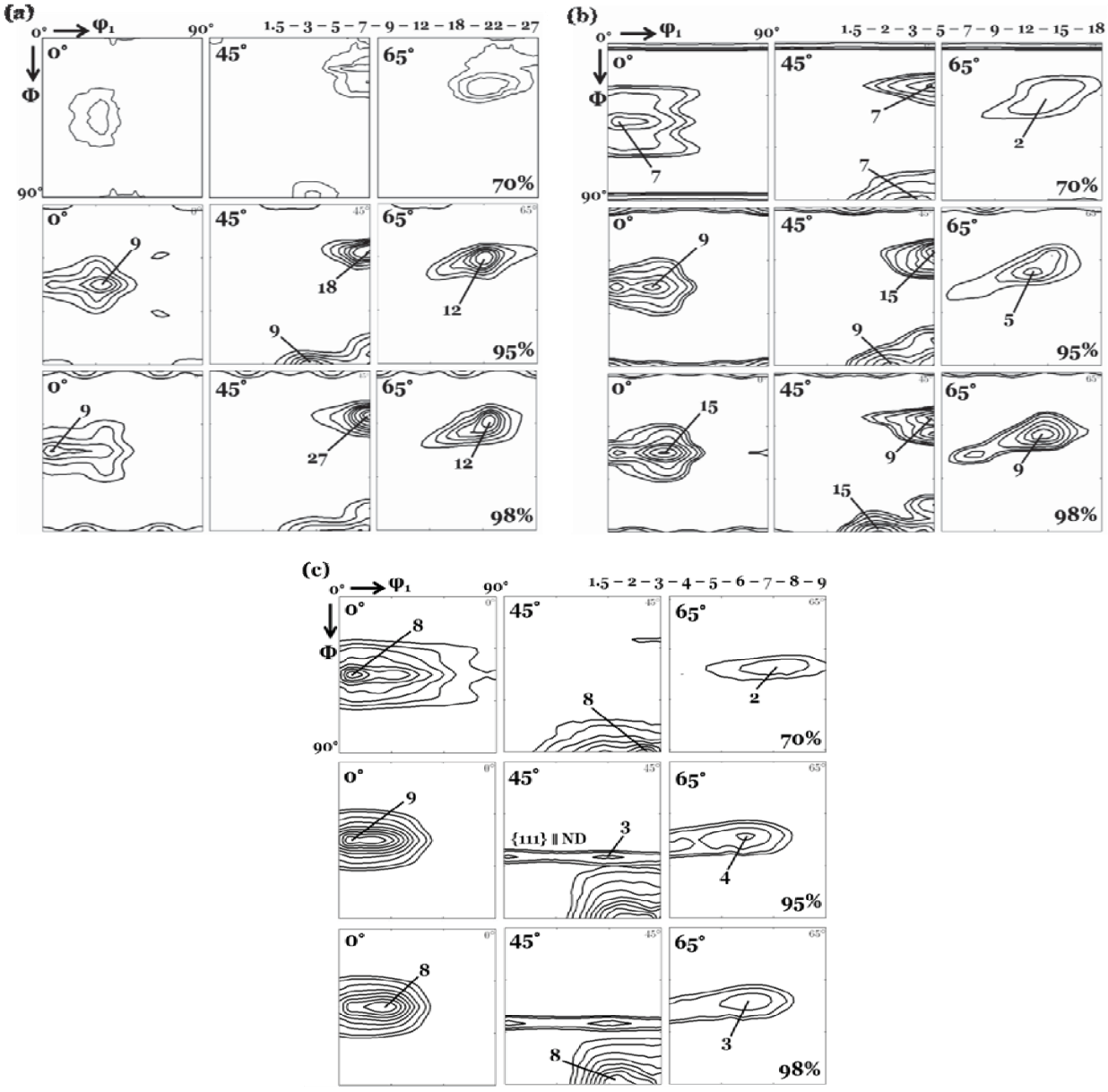

Fig. 1: φ_2 = 0°, 45°, 65° sections of the ODF after 70%, 95% and 98% thickness reductions: (a) pure Al, (b) Al-4Mg, (c) Cu-30Zn.

Unlike in Al and Al-4Mg alloy, the φ_2 = 45° section of the ODF corresponding to 70% reduction in α-brass shows a sudden emergence of <111>‖ND components. However, the intensity of these components decreases with increasing deformation levels. It should be noted that in Al-4Mg alloy the intensity of Cu-

component decreases beyond 95% reduction, which coincides with the corresponding rise in Bs-component.

3.2 Evolution of deformation microstructures

Fig. 2a shows the EBSD generated micrograph of pure Al subjected to 95% thickness reduction. The deformed microstructure is homogeneous and shows a combination of elongated and equiaxed grains. Within the elongated grains, prominent orientation gradients are seen which indicates the presence of intra-granular misorientation. In orientation imaging maps (OIM), these gradients are manifested as color variation within grains. The equiaxed grains are predominantly located adjacent to the prior deformed grains. The presence of a high fraction of high angle grain boundaries (HAGB) indicates the occurrence of restoration mechanisms at high

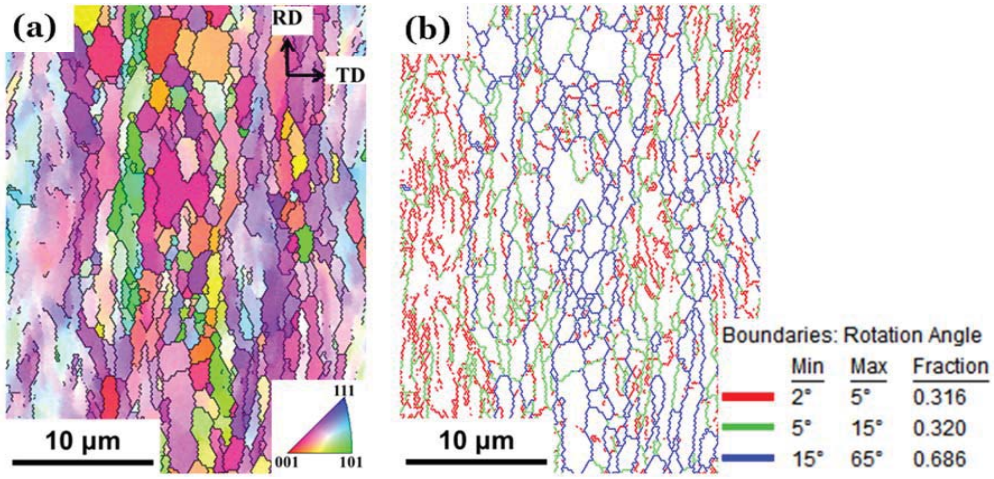

Fig. 2: EBSD generated deformed microstructure of pure Al after 95% thickness reduction: (a) OIM map, (b) grain boundary map.

reductions (Fig. 2b). The deformed micrographs of Al-4Mg alloy subjected to 70% and 90% rolling reductions are given in Fig. 3. The microstructure is homogeneous showing an extensive orientation gradient at 70% reduction (Fig. 3a), whereas after 90% rolling, the onset of shear banding can be observed. The bands are visible as dark patches in the image quality map and are found preferentially in Cu oriented grains (Fig. 3b). These parallel and widely spaced banded features are similar to the ones observed earlier in an Al-Mg alloy by Hurley and Humphreys [21]. They are micro-shear bands (also referred to as Cu-type shear bands) since they are mostly restricted within a grain, and have originated as a result of intense dislocation activity. The dislocation boundaries on either side of the bands show a slight curvature near the interface indicating that the bands cut through the prior sub-grain cells. The area fraction of these bands increases with deformation. In the case of α-brass, the microstructure of 40% rolled condition shows extensive deformation twinning (Fig. 4a). Grains show multiple layers of thin twin lamellae that extend across the grain interior. However, beyond 40% reduction the propensity of twinning almost ceases and band-like feature start to emerge. Similar to Cu-type shear bands, these bands are microscopic, and cut through the pre-existing twin lamellae. However, unlike Cu-type shear bands, these Bs-type shear bands in α-brass are found preferentially within <111>||ND oriented grains (Fig. 4b). The area fraction of Bs-type bands increases with deformation.

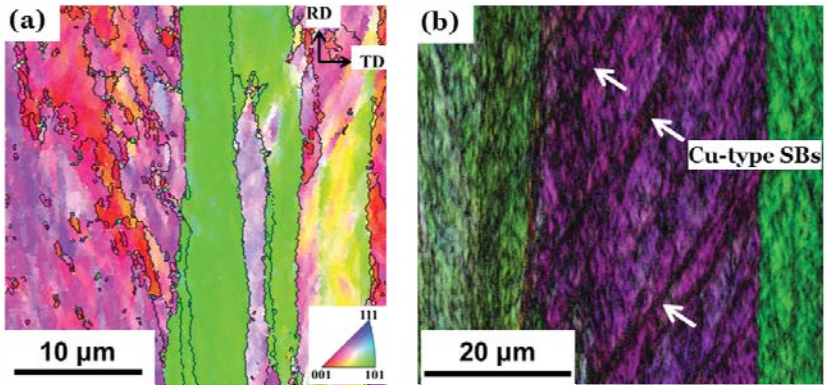

Fig. 3: EBSD generated OIM maps of deformed Al-4Mg alloy after (a) 70% rolled, (b) 90% rolled. Arrows indicate Cu-type shear bands.

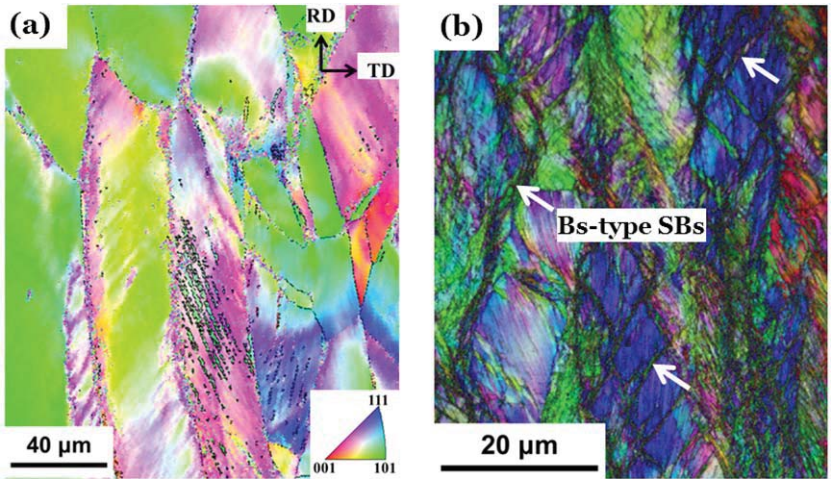

Fig. 4: EBSD generated micrographs of deformed Cu-30Zn alloy. (a) OIM map for 40% rolled, (b) superimposed OIM and image quality maps for 70% rolled. Arrows indicate Bs-type shear bands.

4. Discussion

The clear transition of rolling texture from copper-type to brass-type is evident with decreasing SFE from pure Al to α-brass. The pure Al shows distinct intensity peaks corresponding to Cu, S, and Bs components in the ODF sections. On the other hand, in α-brass, the initial weak texture completely gets transformed to a weak α-fiber texture. It is, therefore, evident that the characteristic evolution of Bs-type texture gets initiated at an early stage of deformation [6]. The Bs-component, which generally constitutes a major fraction of the final texture of low SFE materials, is not seen here as the stable end orientation at large deformation and in turn the intensity maximum is spread throughout the φ_1 values in the $\varphi_2 = 0°$ section (Fig. 1c). This observation is quite contrary to the early reports on the deformation texture of α-brass [5], where a distinct intensity maximum ($f(g)_{max}$) has been observed at Bs location. Nevertheless, this trend is in accordance with our earlier work on Ni-60Co alloy [19], where the $f(g)_{max}$ is not found close to Bs position. Earlier studies [4,5] have indicated that the formation of the Cu-component in the intermediate stages of deformation is crucial in the formation of the final brass-type texture, since this orientation would undergo preferential twinning and subsequent slip to reorient towards the Bs-component. However,

in the present investigation, the fraction of Cu-component is insignificant in the initial material, and no sign of evolution of the Cu-component is evident at any stage of deformation (Fig. 1c). On the other hand, in the medium-SFE Al-4Mg alloy, the texture at a later stage of deformation shows a subtle variation in the intensities of ideal rolling texture components, viz. a decrease in the f(g) of Cu component and a significant rise in the fraction of Bs component.

4.1 Role of SFE in the evolution of microstructure

4.1.1 Pure aluminium

The development of the Cu-type texture in FCC metals is well understood and is generally attributed to cross slip [2]. The microstructures of deformed pure Al indicate the presence of orientation gradients within grains (Fig. 2). These orientation gradients are attributed to predominant dislocation activity as no other deformation mechanism is evident from the microstructures of the rolled materials. The intra-grain misorientation is a result of variation in the slip activity in different parts of the grain, resulting in localized plastic rotation. The sub-division of a grain into smaller domains (sub-grains) subsequent to local rotations is generally accompanied by the formation of low angle boundaries. The orientation spread from the mean orientation of the grain is very high near the triple junctions to account for grain boundary compatibility. However, the condition of boundary compatibilities decreases with increasing deformation due to thinning and elongation of grains. The increase in deformation causes the grains with unstable orientation to converge towards the orientations (like the Cu, S, Bs) which possesses a minimal divergence from its mean position [22].

4.1.2 Al-4Mg alloy

The microstructure and texture development in this alloy is similar to that of other medium SFE materials, viz. pure copper [23]. The deformed microstructure is homogeneous and shows grain fragmentation up to 70% thickness reduction indicating a predominantly dislocation slip based deformation process. The emergence of shear bands in already existing elongated sub-grains is an important observation in the microstructures of large deformation levels. In the present case, these shear bands are confined to single grains, due to the orientation dependence of Cu-type shear bands. Morii et al. [24] have proposed that layered obstacles like lamellar dislocation walls (or microbands) are essential for the initiation of Cu-type shear bands. Under these circumstances, it is relevant to examine the effect of solute atoms on the propensity of shear banding. Earlier studies on Al-Mg and Al-Cu alloys have shown the presence of shear banding at large strains, and the occurrence of shear bands has been attributed to the hindrance of dynamic recovery processes due to the presence of solute atoms (having large atomic misfit) resulting in severe work hardening [12,13]. In a previous work [18], the effect of the evolution of <110>∥ND sub-grains within Cu-type shear bands on the transition of texture has been highlighted. However, in the present case, the influence of Cu-type shear banding and sub-grain evolution within the bands on the copper-type texture is minimal and is least visible in the bulk texture results.

4.1.3 α-brass

(i) Role of twinning

The deformation microstructures indicate a gradual transition in the active modes of deformation i.e., twinning during the initial stages of deformation to shear banding in the later stages. Since the strain accommodation by FCC deformation twins is large (0.707), twin thicknesses are small (20 – 30 nm). Hence, single twin lamellae in EBSD generated OIM micrographs may consist of a bundle of much finer

twins within itself (Fig. 4a). The density of twins within the grains increases with deformation. It can be observed that twins within a grain are parallel to each other, which implies that only one twin variant is active. The formation of twins sub-divides the grains into many fragments which, in effect, would reduce the grain size. The grain size is an important parameter in the nucleation of deformation twins, since it influences the nucleation stress. In the present case, the tendency for twinning got saturated beyond ~40% reduction because of reduced grain size (due to grain fragmentation) and hence higher stress required for further nucleation. In a previous work, Madhavan et al. [19] observed, by a pseudo-in-situ method, a gradual reorientation of twin volumes towards <110>∥ND orientation with increasing deformation, indicating subsequent slip within twin regions.

(ii) Role of shear bands

In the present case, the shear bands are first observed after 50% reduction (ε_t ~ 0.65). The fraction of matrix volume that undergoes banding increases with deformation. The appearance of <111>∥ND components during the later stages is a crucial factor for the origin of shear bands in the microstructure. The formation of these {111} components can be explained as follows [25]: subsequent to deformation twinning, dislocation slip is largely confined to slip planes that are parallel to the twin habit planes. Slip will remain active till the twin plane (slip plane) rotates towards the rolling plane of the sample, beyond which the resolved stress acting on the slip plane is very low. The rotation of twin lamellae parallel to the rolling plane suppresses homogeneous crystallographic slip making the microstructure plastically unstable. The subsequent evolution of shear bands is the outcome of this plastic instability [16]. Fig. 4b depicts the situation where banding is extensive in one of the <111>∥ND oriented grains and is cutting through pre-existing twins. The orientation of sub-grains within the shear band is of particular interest since it could play an influential role in deciding the final rolling texture. A careful examination of regions within the shear bands indicates that the distribution of crystallite orientations is not random, but preferentially towards <110>∥ND.

5. Conclusions

An understanding of the evolution of texture and microstructure in pure Al, Al-4Mg and α-brass with stacking fault energies ranging from high to low has been developed. The key observations are as follows:

1. Pure aluminium develops a characteristic copper-type rolling texture at large rolling reductions comprising high fractions of S, Bs and Cu components. The evolution of texture in this material is primarily attributed to dislocation slip as evidenced by intense dislocation activity throughout the deformation.

2. In Al-4 wt.% Mg alloy, the overall texture is copper-type up to 98% reduction (ε_t = 3.9). The deformation mechanism up to a thickness reduction of ~70% is entirely slip-dominated. Beyond this deformation level, the initiation of Cu-type shear bands is observed. These shear bands are mostly confined to {112}<111> oriented grains. The effect of shear bands and the subsequent sub-grain evolution within the bands are least visible in the macro-texture of this alloy.

3. α-brass develops a characteristic brass-type rolling texture and the development of this texture starts in the early stages of deformation (ε_t ~ 0.5). The volume fraction of the Cu {112}<111> component is insignificant during the entire process of deformation. A clear transition in the deformation mechanisms from extensive deformation twinning in the intermediate stages (ε_t < 0.5) to shear banding in the later stages is observed. The major orientation changes towards the α-fiber, in the intermediate stages of deformation, take place by extensive twinning and slip within the twin volumes. In the later stages of

deformation, shear bands originate due to plastic instability caused by the emergence of <111>||ND components in the microstructure. A non-random distribution of orientations close to <110>||ND orientation is found inside the shear bands.

References

[1] T. Leffers and R.K. Ray 2009 *Prog. Mater. Sci.* **54** 351-396.
[2] R.E. Smallman and D. Green 1964 *Acta Metall.* **12** 145-154.
[3] W. Heye and G. Wassermann 1966 *phys. stat. solidi (b)* **18** 107-111.
[4] J.S. Kallend and G.J. Davies 1972 *Texture* **1** 51-69.
[5] J. Hirsch and K. Lücke 1988 *Acta Metall.* **36** 2863-2882.
[6] T. Leffers and D.J. Jensen 1988 *Text. Microstruct.* **8** 467-480.
[7] T. Leffers 1993 *Text. Microstruct.* **22** 53-58.
[8] T. Leffers 1996 *Proc. ICOTOM 11* **1** 299-306.
[9] P. Wagner, O. Engler and K. Lücke 1995 *Acta Metall. Mater.* **43** 3799-3812.
[10] K. Morii, H. Mecking and Y. Nakayama 1985 *Acta Metall.* **33** 379-386.
[11] O. Engler 2000 *Acta Mater.* **48** 4827-4840.
[12] O. Engler, J. Hirsch and K. Lücke 1989 *Acta Metall.* **37** 2743-2753.
[13] P. Wagner, O. Engler and K. Lücke 1991 *Text. Microstruct.* **14-18** 927-932.
[14] T.C. Kamijo and K. Sekine 1970 *Metall. Mater. Trans. B* **1** 1287-1292.
[15] P.T. Wakefield, A.S. Malin and M. Hatherly 1977 *J. Aust. Inst. Met.* **22** 143-151.
[16] B.J. Duggan, M. Hatherly, W.B. Hutchinson and P.T. Wakefield 1978 *Met. Sci.* **12** 343-351.
[17] W.B. Hutchinson, B.J. Duggan and M. Hatherly 1979 *Met. Technol.* **6** 398-403.
[18] R. Madhavan, R.K. Ray and S. Suwas 2014 *Acta Mater.* **74** 151-164.
[19] R. Madhavan, R.K. Ray and S. Suwas 2014 *Acta Mater.* **78** 222-235.
[20] H. Schaeben, R. Hielscher and F. Bachmann 2010 *Solid State Phenom.* **160** 63-68.
[21] P.J. Hurley and F.J. Humphreys 2003 *Acta Mater.* **51** 1087-1102.
[22] Y. Zhou, L.S. Tóth and K.W. Neale 1992 *Acta Metall. Mater.* **40** 3179-3193.
[23] J. Hirsch, K. Lücke and M. Hatherly 1988 *Acta Metall.* **36** 2905-2927.
[24] K. Morii and Y. Nakayama 1985 *Scr. Metall.***19** 185-188.
[25] T. Leffers 1978 *ICOTOM 5* **1** 277-287.